Temperature Dependence of the Optical Constants of Tantalum Nitride formed by Atomic Layer Deposition on 300 mm wafers

MASTER'S DEFENSE

Aaron Lopez Gonzalez

College of Arts and Sciences   Department of Physics

BE BOLD. Shape the Future.®
New Mexico State University

Acknowledgements

- **COMMITTEE:**
  - Dr. Stefan Zollner
  - Dr. Matthew Sievert
  - Dr. Jason Jackiewicz

- **COLLABORATORS:**
  - Ekta Bhatia, *NY CREATES*
  - Tuan Vo, *NY CREATES*
  - Satyavolu Papa Rao, *NY CREATES*

- **RESEARCH PEERS:**
  - Yoshitha Hettige
  - Carlos Armenta
  - Sonam Yadav
  - Jaden Love
  - Haley Woolf
  - Gabriel Ruiz

- **FUNDING:**
  - Louis Stokes Alliance for Minority Participation *(HRD 1826758)*
  - Air Force Office of Scientific Research *(FA9550-20-1-0135, FA9550-24-1-0061)*
  - Air Force Research Laboratory, Rome, NY *(FA8750-19-1-0031, FA8649-21-P-0773)*

Vita:

2022-2024: **Peer mentor**
NMSU - STAR Program

2022-2024: **Undergraduate Research Assistant**
NMSU

2023: **REU Astrophysics**
Villanova University/LIGO

2024: **B.S. Engineering Physics**
NMSU

2024-2025: **Graduate Teaching Assistant**
NMSU

2025: **Graduate Research Assistant**
NMSU

Posters:

A. Lopez Gonzalez, and S. Zollner, *Standard error measurements of Si, SiO2, and TaN wafers for band gap determination*, URCAS 2023, Las Cruces, NM, USA, April 14th, 2023.

A. Lopez Gonzalez, and A. L. Stuver, *The Impact of Gravity Spy Glitch Classes on a Search for Burst Gravitational Waves*, AstroPhilly23, Villanova, PA, USA, July 27th, 2023.

A. Lopez Gonzalez, and S. Zollner, *Optical constants of Tantalum Nitride from 0.03 eV to 6.5 eV at different temperatures*, 2023 NM AMP Student Research Conference, Las Cruces, NM, USA, October 13th, 2023.

A. Lopez Gonzalez, Y. Hettige, J. R. Love, S. Zollner, E. Bhatia, T. Vo, and S. P. Rao, *Dielectric function of Tantalum Nitride formed by atomic layer deposition on 300 mm wafers*, AVS 69th International Symposium & Exhibition, Portland, OR, USA, November 7th, 2023.

A. Lopez Gonzalez, and A. L. Stuver, *The Impact of Gravity Spy Glitch Classes on a Search for Burst Gravitational Waves*, 243rd AAS meeting, New Orleans, LA, USA, January 6th, 2024.

A. Lopez Gonzalez, Y. Hettige, J. R. Love, S. Zollner, E. Bhatia, T. Vo, and S. P. Rao, *Temperature Dependence of the Dielectric Function of Tantalum Nitride Formed by Atomic Layer Deposition*, 10th International Conference on Spectroscopic Ellipsometry, Boulder, CO, USA, June 12th, 2025.

Presentation:

A. Lopez Gonzalez, Y. Hettige, J. R. Love, S. Zollner, E. Bhatia, T. Vo, and S. P. Rao, *Dielectric Function of Tantalum Nitride Formed by Atomic Layer Deposition on 300 mm Wafers for Josephson Junction Applications*

APS Global Physics Summit 2025, Anaheim, CA, USA March 19th, 2025.

Awards

J.A. Woollam Co., Inc. Outstanding Undergraduate Student Poster Presentation

"Dielectric function of Tantalum Nitride formed by atomic layer deposition on 300 mm wafers"

AVS 69th International Symposium & Exhibition

November 7th, 2023

Outline

- **General theory and methods**
  - Electronic Band Structure
  - Theory of Spectroscopic Ellipsometry
  - Instrumentation
  - Data analysis method
- **Measurement of tantalum nitride on Si/SiO_2 using X-Ray reflectance**
  - Methods
  - Results
- **Temperature-dependent dielectric function of tantalum nitride formed by atomic layer deposition for tunnel barriers in Josephson Junctions**
  - Results and Discussion
  - Conclusion
- **Outlook and Summary**

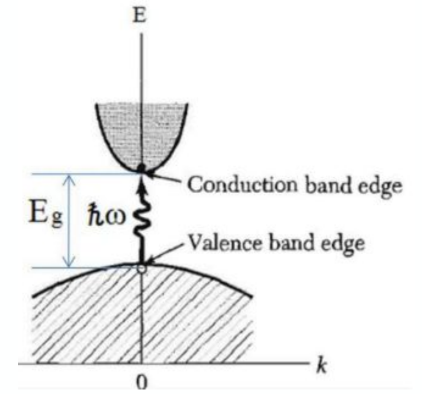

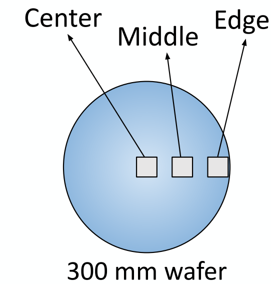

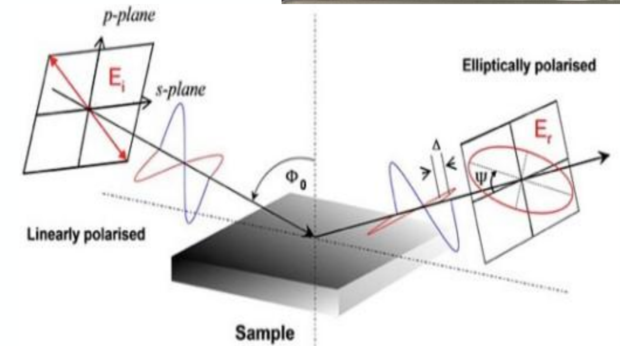

BE BOLD. Shape the Future.®

Motivation

- We report the dielectric functions of insulating tantalum nitride (TaN) films, deposited using atomic layer deposition (ALD) on 300 mm Si/SiO_2 substrates, *to demonstrate their suitability as tunnel barriers* in tantalum-based Josephson junctions for superconducting quantum circuits.
- Compared to aluminum oxide barriers, we expect ALD TaN to show *improved thermal stability and resistance to aging.*
- The lower band gap of TaN suggests the possibility of fabricating Josephson junctions with *thicker barriers* while achieving critical current densities required for qubits, *better control of thickness and composition*, and *reduced defect densities.*
- These characteristics show the potential of ALD TaN as a Josephson junction tunnel barrier that can *improve the reliability and performance* of superconducting quantum computing circuits.
- Ellipsometric measurements on these TaN films allows us to measure the *band gap and optical constants*.

General theory and methods

Introduction

For TaN thin films, ellipsometry allows characterization of how the refractive index and extinction coefficient vary with wavelength and temperature. Since TaN is of interest for electronic, optical, and protective applications, understanding its optical constants is essential for device design and for understanding its fundamental electronic structure.

We'll briefly touch on four main sections:

1. The **electronic band structure**,
2. The **theory of spectroscopic ellipsometry**,
3. The **instrumentation** used, and
4. The **sample preparation and data analysis** methods.

Electronic band structure

To understand a material's optical properties, we must first look at its **electronic band structure**.
In a single atom, electrons occupy discrete energy levels. But when many atoms come together to form a solid, these levels broaden into **energy bands** — separated by **band gaps** where no electronic states exist.

- **Metals** have partially filled bands — hence they conduct electricity easily.

- **Semiconductors and insulators** have band gaps.
  If the gap is small, around 1–3 eV, we call it a semiconductor.
  If it's larger, typically above 4 eV, it behaves as an insulator.

This framework explains how **light absorption** and **electronic transitions** occur in Tantalum nitride.

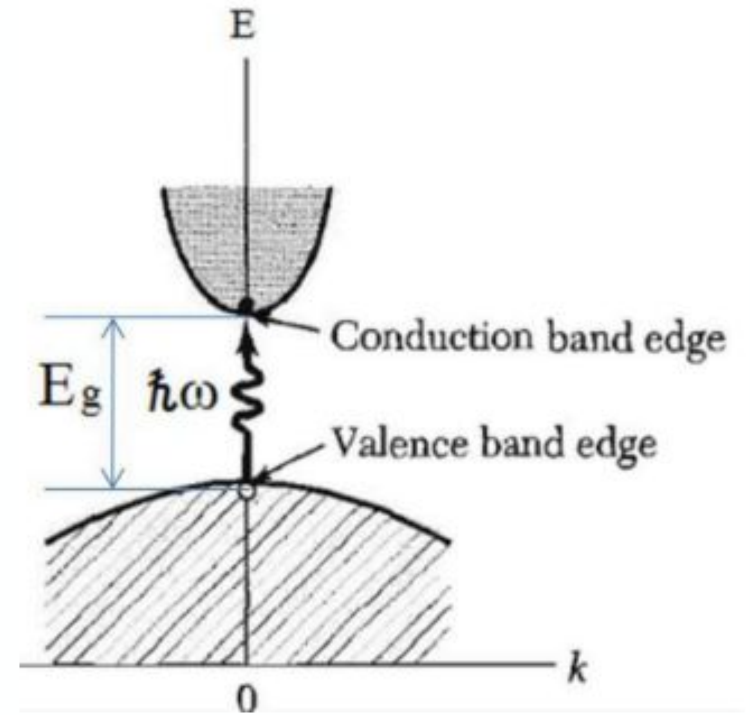

A band gap is the energy difference between the top of the valence band and the bottom of the conduction band in a solid, with ħω being the energy required to excite an electron from the valence band to the conduction band.

I. Kaplan, (John Wiley & Sons, Chichester, 2017) pp. 25, 27.
M.H. Saleh, Study of Structural, Optical and… (2011).
J. Gusakova, B.K. Tay, and V. Gusakov, Phys. Status Solidi A, 1–4 (2016).

Density of States

Another key concept is the density of states (DOS), which specifies the number of electronic states available at a given energy. The DOS plays a central role in determining the electronic, thermal, and optical properties of a material. Optical transitions are allowed between states in the valence band and states in the conduction band if energy and momentum conservation conditions are satisfied.

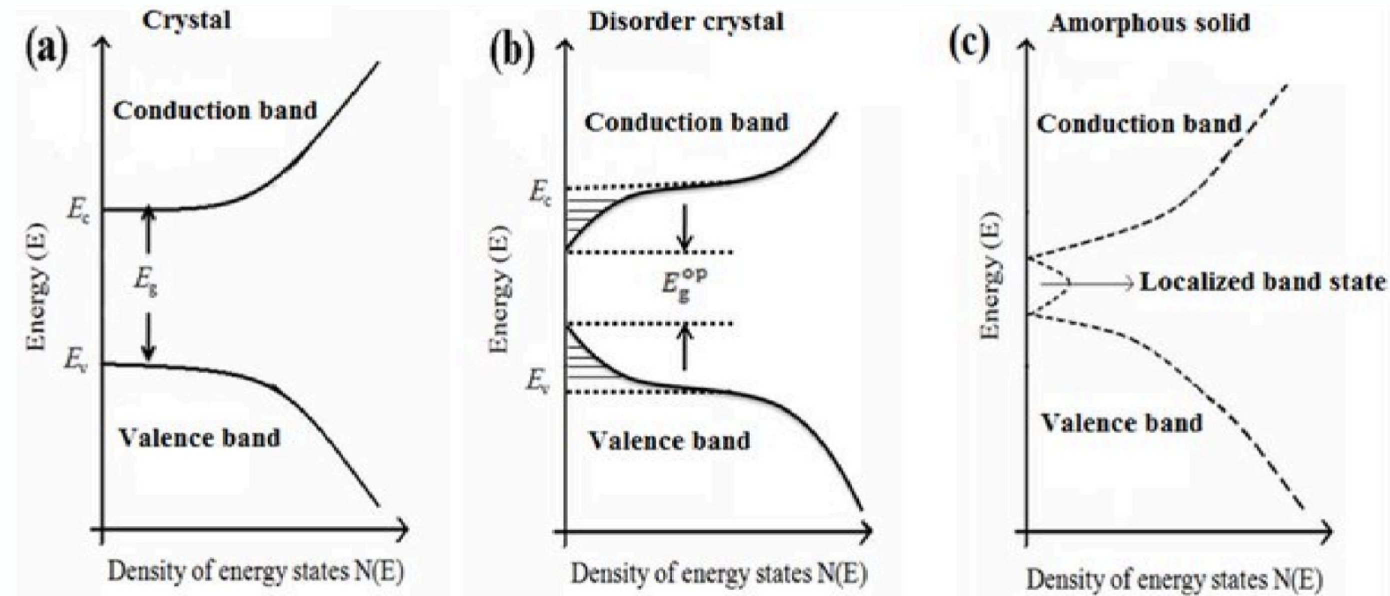

Spectroscopic Ellipsometry (SE) measures the dielectric function, which is a direct consequence of the material's electronic band structure. The key features of the dielectric function are physically rooted in the DOS, meaning SE can be used to probe and confirm a material's electronic structure.

The density of states is valid only for free electrons, meaning that electrons in a solid are not free, and the density of states is zero inside the band gap. Image shows a schematic diagram of the band-structure density of states as a function of energy for crystalline (a), disordered (b) and amorphous solid materials (c).

M.H. Saleh, Study of Structural, Optical and… (2011).
W. Tausendfreund, J. Phys. C: Solid State Phys, 8 (7), 1000-1009 (1975).

Optical properties and Band structure

The optical constants of a material, namely the refractive index *n* and the extinction coefficient *k*, are intimately related to its electronic band structure. The *n* and *k* are the real and imaginary parts of the complex refractive index *ñ*:

$$\tilde{n} = n + ik$$

This *ñ* relates to the complex dielectric function $\tilde{\varepsilon}(\omega)$:

$$\tilde{\varepsilon}(\omega) = \varepsilon_1(\omega) + i\varepsilon_2(\omega) = \tilde{n}^2 = (n + ik)^2$$

So, the optical constants *n* and *k* are derived directly from the dielectric response of the material, and this dielectric function $\tilde{\varepsilon}(\omega)$ describes how the material's electrons respond to an electromagnetic field (light). It has two main components related to the electronic band structure:

$$\varepsilon_1 = n^2 - k^2$$

$$\varepsilon_2 = 2nk$$

1. Interband Transitions — electrons absorb photons and jump between the valence and conduction bands.
2. Intraband (Free Carrier) Transitions — conduction electrons respond to low-energy fields (dominant in metals).

Index of Refraction: $n = {}^{c}/_{v}$

Extinction Coefficient: $k = \alpha \frac{\lambda}{4\pi}$

A.R. Forouhi, I. Bloomer, HOCSi, 2, 151-175 (1997).

Optical properties and Band structure pt.2

The **refractive index *n*** and **extinction coefficient *k*** form what's known as the **complex refractive index**, represented as ***n* + *ik***.
These are directly related to the **complex dielectric function**, which tells us how electrons in a material respond to light.

In essence:

- The **real part** (*n*) describes how fast light travels through the material, and
- The **imaginary part** (*k*) describes how much light is absorbed.

By measuring *n* and *k* across different photon energies and temperatures, we can learn about the **band gap**, **transition energies**, and even the **degree of disorder** in the TaN films.

A.R. Forouhi, I. Bloomer, HOCSi, 2, 151-175 (1997).

Principles of Ellipsometry

Ellipsometry is based in the understanding that light is an electromagnetic wave interacting with materials. Because of this, it provides an optical technique used to determine the dielectric properties (complex refractive index or dielectric function) of thin films. Ellipsometry measures changes in the polarization state of light after reflection from or transmission through a material.

$$\rho = \frac{r_p}{r_s} = \frac{E_{rp}/E_{ip}}{E_{rs}/E_{is}} = \tan\psi e^{i\Delta} \quad \text{Fresnel coefficients}$$

$$r_p = \frac{E_{rp}}{E_{ip}} = \frac{n_t cos(\theta_i) - n_i cos(\theta_t)}{n_t cos(\theta_i) + n_i cos(\theta_t)}$$

$$r_s = \frac{E_{rs}}{E_{is}} = \frac{n_i cos(\theta_i) - n_t cos(\theta_t)}{n_i cos(\theta_i) + n_t cos(\theta_t)}$$

Amplitude Ratio: $\tan(\Psi) = \left|\frac{r_p}{r_s}\right|$

Phase Difference: $\Delta = \delta_p - \delta_s$

$$\langle\varepsilon\rangle = sin^2(\theta_i)[1 + tan^2(\theta_i)(\frac{1-\rho}{1+\rho})^2]$$

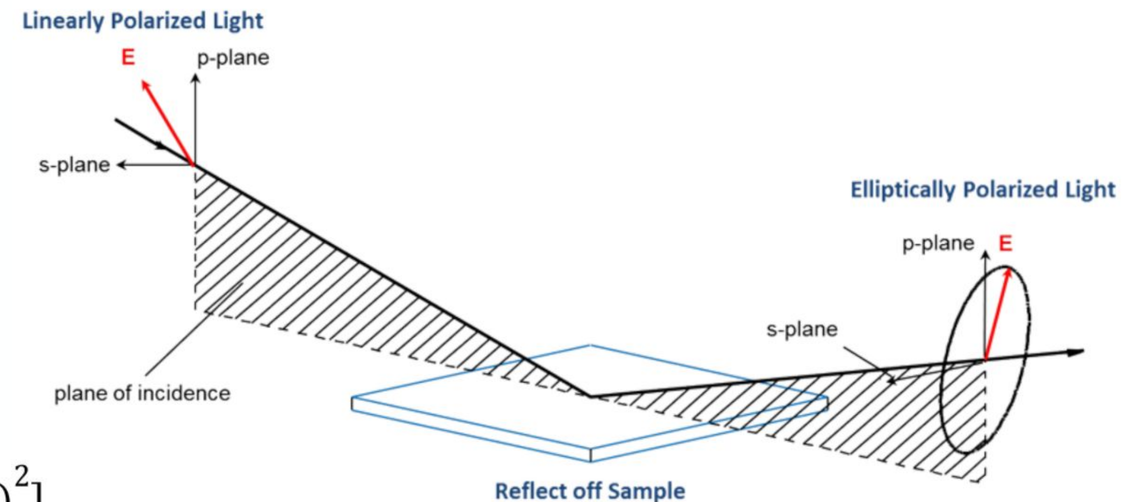

K. Vedam, Thin Solid Films 313–314, 1–9 (1998).
G.E. Jellison, Thin Solid Films, 234, 416-422 (1993).
J.A. Woollam, Ellipsometry FAQ, website (Accessed July 20, 2025).

Principles of Ellipsometry pt. 2

Ellipsometry measures the ratio of the amplitude reflection coefficients r_p/r_s, and since the difference between r_p and r_s is maximized at the Brewster angle, sensitivity for the measurement also increases at this angle.

The Brewster angle is the specific angle at which the light completely polarizes. When unpolarized light is incident on a flat surface, the reflected light partially polarizes to the plane of the refractive index. This complete polarization with the Brewster angle occurs when the reflected and refracted rays are perpendicular to one another. This can be explained by using Snell's law:

$$n_1 \sin\theta_1 = n_2 \sin\theta_2$$

$$\theta_B + \theta_2 = 90^o \; -> \; \theta_2 = 90^o - \theta_B$$

$$\sin\theta_2 = \sin(90^o - \theta_B) = \sin 90^o \cos\theta_B - \cos 90^o \sin\theta_B$$

$$\sin\theta_2 = \cos\theta_B$$

$$n_1 \sin\theta_B = n_2 \cos\theta_B$$

$$\tan\theta_B = \frac{n_2}{n_1} \Rightarrow \theta_B = \tan^{-1}\left(\frac{n_2}{n_1}\right)$$

The brewster angle and index of refraction of TaN was unknown, so we took ellipsometric measurements at room temperature for incident angles of 50° to 80° to account for the known brewster angles of Si and SiO_2, which are approximately 75° and 55°, respectively.

H. Fujiwara, Spectroscopic Ellipsometry… (John Wiley & Sons, Chichester, 2007) pp. 37, 40.
D. Amrani, J. Sci. Educ., 23 (1), 41 (2022).

Spectroscopic Ellipsometry

In spectroscopic ellipsometry, measurements are taken across a broad wavelength or photon energy range, typically from the ultraviolet (UV) to the infrared (IR). This spectral information provides insight into the electronic transitions, absorption edges, and dispersion behavior of the material.

Advantages:

- High sensitivity to film thicknesses
- Ability to characterize both *n* and *k*
- Non-destructive and contactless procedure

Disadvantages:

- Does not provide optical constants directly
- Does not measure film thickness for thin layers
- Requires model-based analysis with assumptions

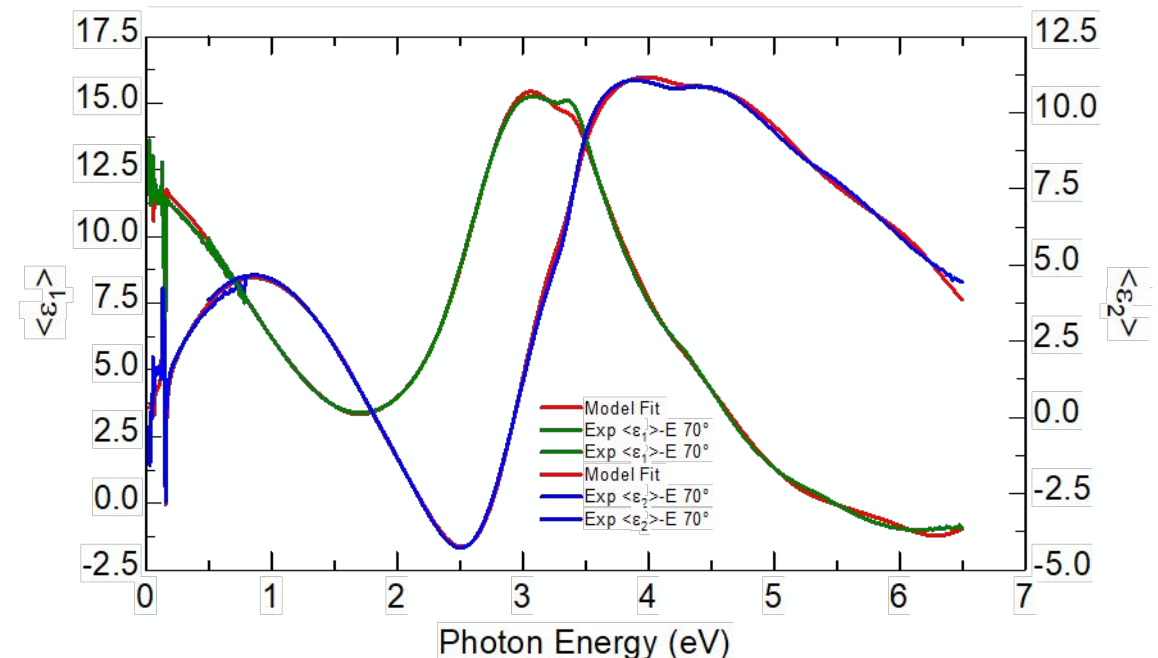

G.E. Jellison, Thin Solid Films, 234, 416-422 (1993).

Dielectric function models - Tauc-Lorentz

Mathematical formula that describes the optical properties of amorphous materials like semiconductors. It is used to fit the complex refractive index of amorphous materials at frequencies greater that their optical band gap. It includes both a sharp optical absorption edge and a tail below the band gap, so it accounts for sub-bandgap absorption (band tail), unlike Lorentz model which is symmetric.

The *Tauc joint density of states (JDOS) model* relates the material's absorption coefficient (α) to the available energy states for electron transitions. Accounts for band-to-band absorptions.

The *classical Lorentz oscillator* model is a physical model that describes the optical response of a material by treating its electrons as damped harmonic oscillators - the absorption peaks in a material.

$$\varepsilon = 1 + \Sigma \frac{A_j E_{0j}}{E_{0j}^2 - E^2 + i\Gamma E_n}$$

A is amplitude
Eo is peak transition energy
Subscript j indicates jth oscillator
E is the energy at that point
Γ is the damping coefficient

$$\varepsilon_2 = \frac{A E_o C (E_n - E_g)^2}{(E_n^2 - E_o^2)^2 + C^2 E_n^2} \frac{1}{E_n} \quad \text{for } E_n > E_g$$

A is amplitude
Eo is peak transition energy
Eg is band gap energy
C is broadening term for the model

$$(\alpha\hbar\omega)^{1/n} = B(\hbar\omega - E_g)$$

α - absorption coefficient
hw - photon energy
B - material constant
n - exponent that characterizes type of electronic transition
n=2 for allowed direct transitions; n=½ for allowed indirect transitions

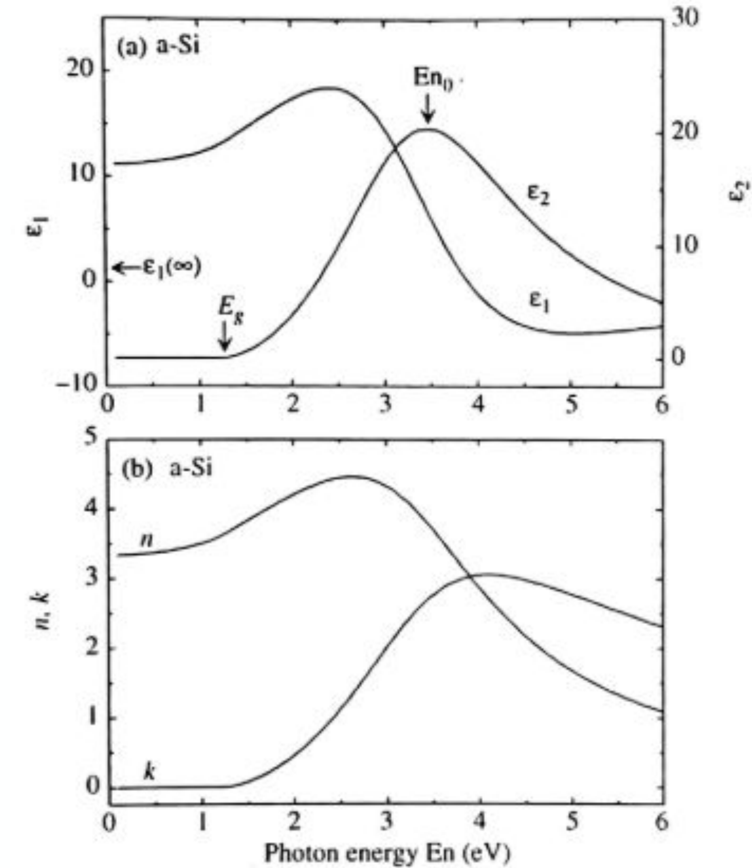

(top) Dielectric function and (bottom) (*n*, *k*) spectra of an amorphous silicon calculated from Tauc-Lorentz model.

G.E. Jellison, Thin Solid Films, 234, 416-422 (1993).

Instrumentation

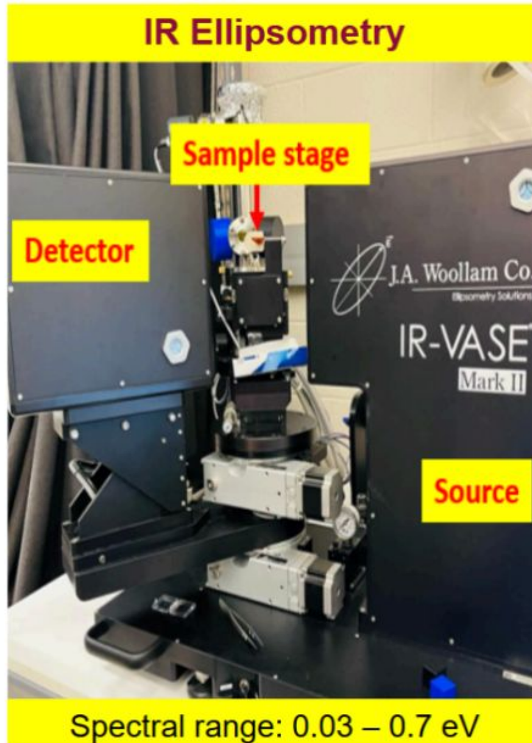

This IR ellipsometer has the ability to probe vibrational modes and free carrier absorption in material, as well as having high accuracy in determining optical constants in the mid-IR region.

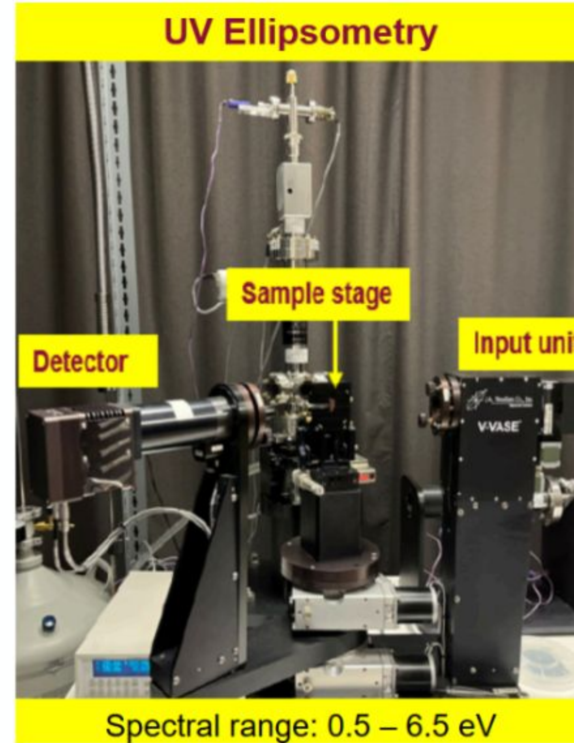

Capable of detecting interband electronic transitions and absorption edges with high sensitivity, obtaining high spectral resolution across a broad UV-Vis-NIR range, measuring ultrathin films and multilayer structures.

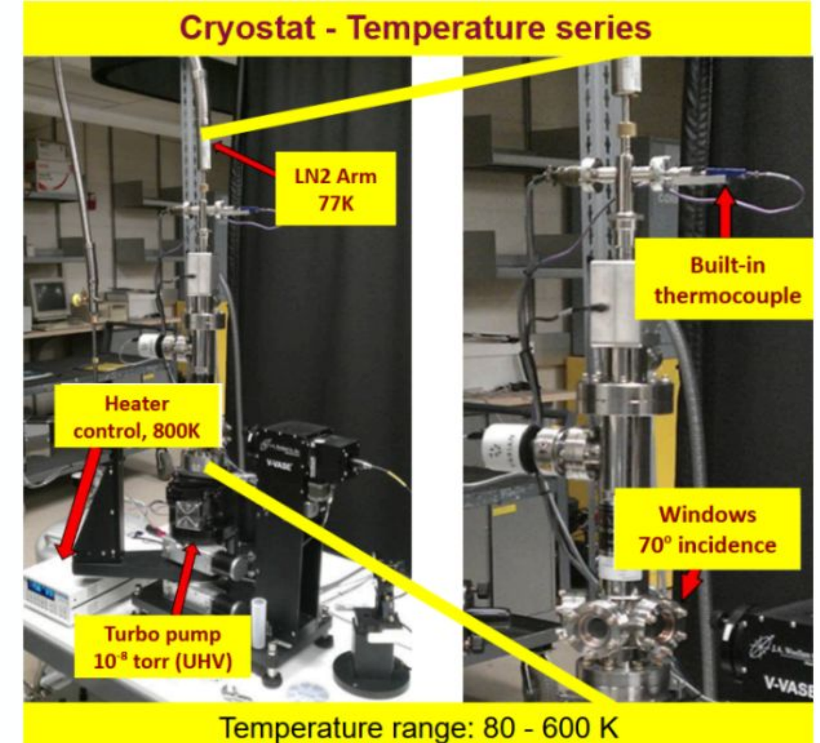

Precise temperature control down to ~10 K with optical access for measurements. Its UHV design minimize contamination, and its window ports enable broad spectral measurements, making it ideal for studying the temperature-dependent optical properties of thin films.

J.A. Woollam, IR-VASE Mark II Ellipsometer, website (Accessed July 21, 2025).
J.A. Woollam, VASE Ellipsometer, website (Accessed July 21, 2025).
Lake Shore Cryotronics, ST-400 Series ultra-high vacuum cryostats, website (Accessed July 22, 2025).

Data analysis methods

1. Acquire Ψ and Δ spectra from both the IR-VASE and VASE instruments using W-VASE software.

2. Import the measured data into W-VASE for initial model fitting and parameter extraction.

3. Once the best model was created following the ε_1 and ε_2 data, export processed data to Microsoft Excel for tabular organization and for the expression of graph points.

4. Use OriginPro to generate publication-quality plots.

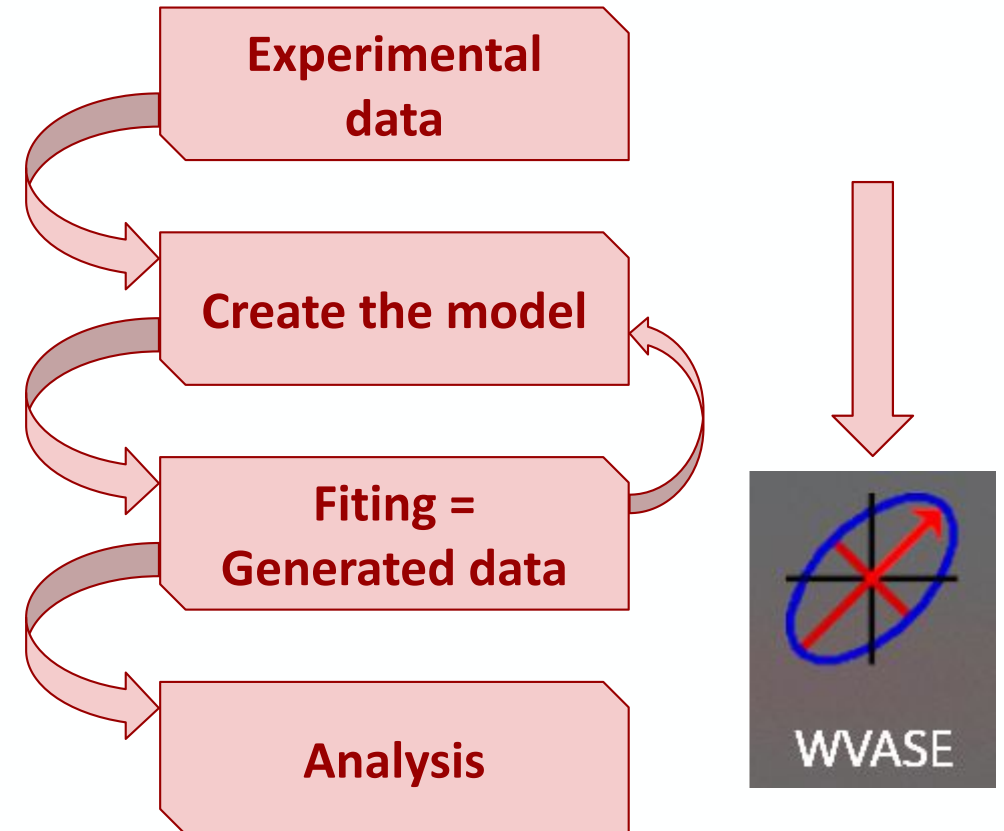

J.A. Woollam, WVASE, website (Accessed July 22, 2025).

Sample preparation methods

3 -> Si / SiO_2 44 nm (post Ar sputter) / TaN 25 nm
3 -> Si / SiO_2 44 nm (post Ar sputter) / TaN 12 nm
3 -> Si / SiO_2 44 nm (post Ar sputter)
1 -> Si / SiO_2 50 nm (as grown)
1 -> Si substrate

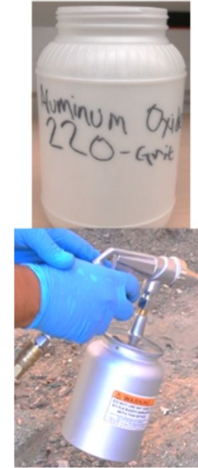

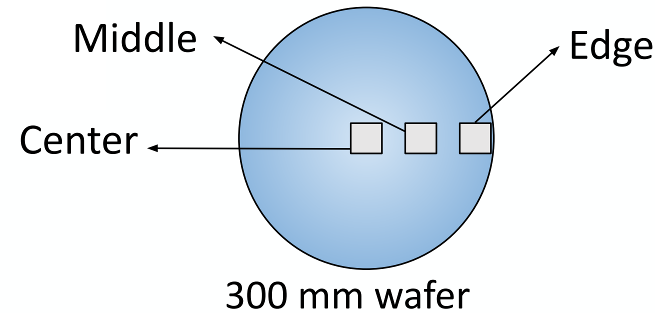

Conclusion

- The electronic band structure of solids provides the foundation for understanding the optical response of materials, while spectroscopic ellipsometry offers a powerful means of experimentally probing these optical constants across broad spectral ranges.
- The instrumentation used, IR-VASE and VASE ellipsometers controlled via W-VASE software, enabled precise measurements.
- Data was further organized in Excel and presented graphically using OriginPro.
- Careful sample preparation was performed to ensure reliable measurements, including ultrasonic cleaning and sandblasting to remove back-side reflections. This project used a set of 11 samples with different configurations of TaN and SiO_2 layers on Si substrates prepared by ALD.
- Together, these theoretical and methodological elements form the basis for the investigation of the optical constants and temperature dependence of tantalum nitride thin films, presented in the following chapters.

Measurement of tantalum nitride on Si/SiO_2 using X-Ray reflectance

Introduction

Thickness, density and roughness of layers on a substrate can be determined via X-Ray Reflectance (XRR), which basically detects the reflections of X-Rays as the incident angle changes. Total external reflection for angles small enough.

The index of refraction of the sample is: $n = 1 - \delta + i\beta$ where beta is the attenuation of the material and delta the dielectric polarization:

$$\delta = \frac{N_A Z r_{el} \rho}{2\pi A}\lambda^2$$

Z - atomic number, A - mass of element, p - mass density

At critical angle, X-Rays are refracted parallel to the interface of air and material, reducing Snell's law to the cos(alpha)=n. After Taylor expansion:

$$\theta_{crit} \approx \sqrt{2\delta}$$

$$r_p = \frac{E_{rp}}{E_{ip}} = \frac{n_t cos(\theta_i) - n_i cos(\theta_t)}{n_t cos(\theta_i) + n_i cos(\theta_t)}$$

$$r_s = \frac{E_{rs}}{E_{is}} = \frac{n_i cos(\theta_i) - n_t cos(\theta_t)}{n_i cos(\theta_i) + n_t cos(\theta_t)}$$

An X-ray beam is directed at a sample at very low angles, called "grazing angles":

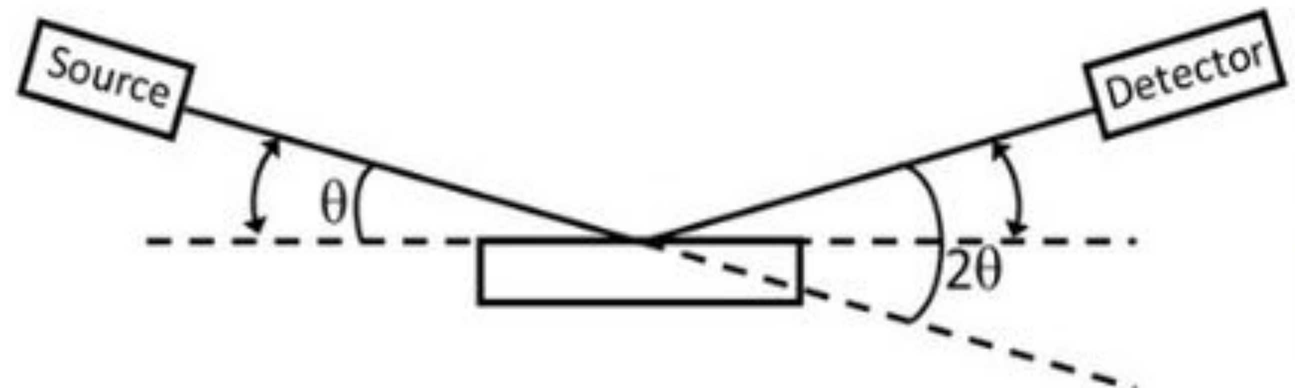

E. Chason and T. M. Mayer, CRSSMS, 22 (1), 1-67 (1997).
A. Gibaud et al, "X-Ray Reflectivity", Surface Science Techniques (pp. 191-216), Heidelberg, 2013.
A. Gibaud and S. Hazra, Current Science, 78 (12), 1467-1477 (2000).

Introduction pt. 2

Constructive: Bragg's law is satisfied: $n\lambda = 2d\sin\theta$ when the length difference of reflected waves is an integer multiple of the X-ray wavelength ($n\lambda$).

Destructive: Reflected waves cancel each other when their length difference is a half-integer multiple of the X-ray wavelength ($(n+1/2)\lambda$).

- At each interface where there is a change in electron density, a portion of the X-ray beam is reflected, and another is refracted and transmitted to the next layer
- The reflected beams from these interfaces travel different path lengths before reaching the detector
- The phase difference between these reflected waves determines if they interfere **constructively** or **destructively**
- Constructive and destructive interference are what produce the characteristic oscillation patterns in the measured data, called *Kiessig fringes*
- We can relate the frequency of these oscillations to the thickness by looking at the period of 2π completed by each oscillation

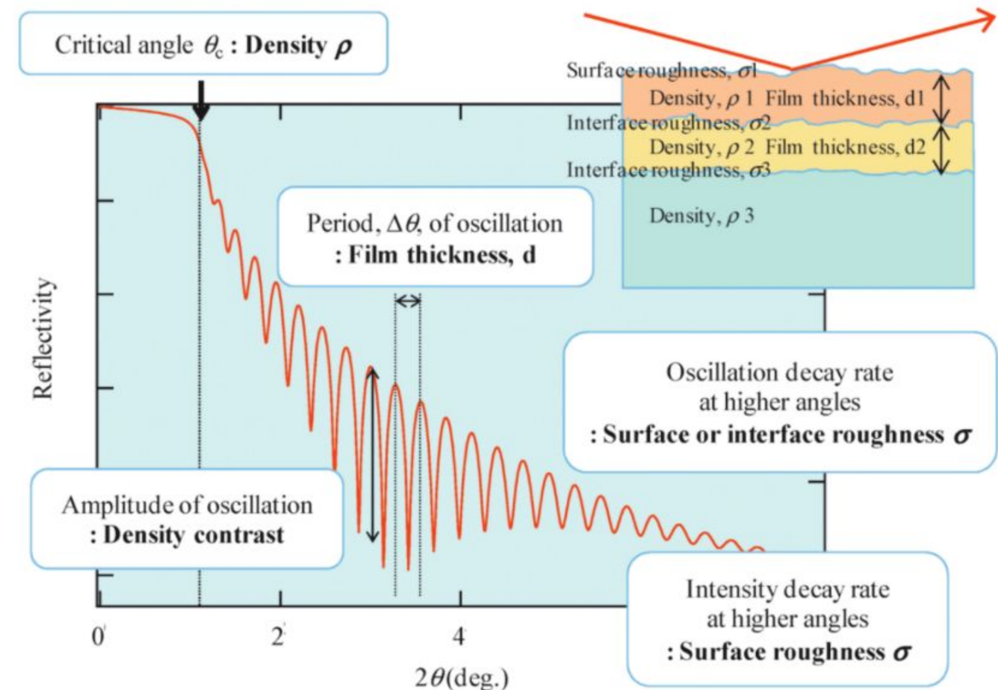

The thickness of the layer expressed in reciprocal space is given by:

$$T = \frac{2\pi}{\Delta Q}$$

BE BOLD. Shape the Future.®

M. Yasaka, The Rigaku Journal, 26 (2), 1-9 (2010).
J. P. Sauro, J. Bindell, and N. Wainfan, Phys. Rev., 143 (2), 439-443 (1966).
M. R. Sardela, Practical Materials Characterization (pp. 1-41), Media New York, 2014.

Methods

To determine the range of 2θ to be used, a fast scan was performed on the sample.

This scan showed that a range of 0º to 5º was the best option since the first range selected (0º to 3º) was not showing the entire XRR pattern.

Once we knew the range of 2θ we needed to use, we ran a long scan.

Hybrid monochromator 2xGe(200) for Cu	Soller slits 0.04 rad
Fixed divergence slit of 1/32º	Xenon proportional detector
Fixed mask of 10 mm	Nickel beam attenuator of 0.125 mm
Parallel plate collimator slit	Parallel plate collimator of 0.27º

$Si/SiO_2/TaN$ films from 300 mm wafer

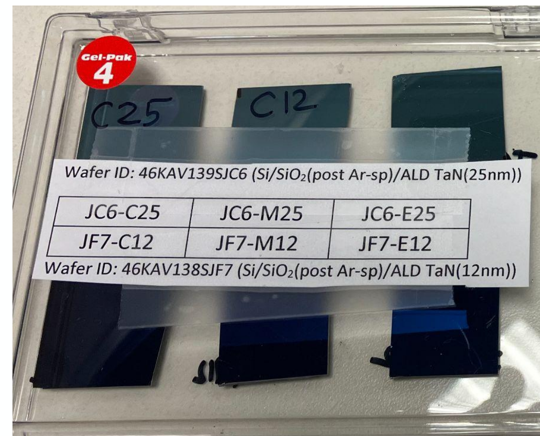

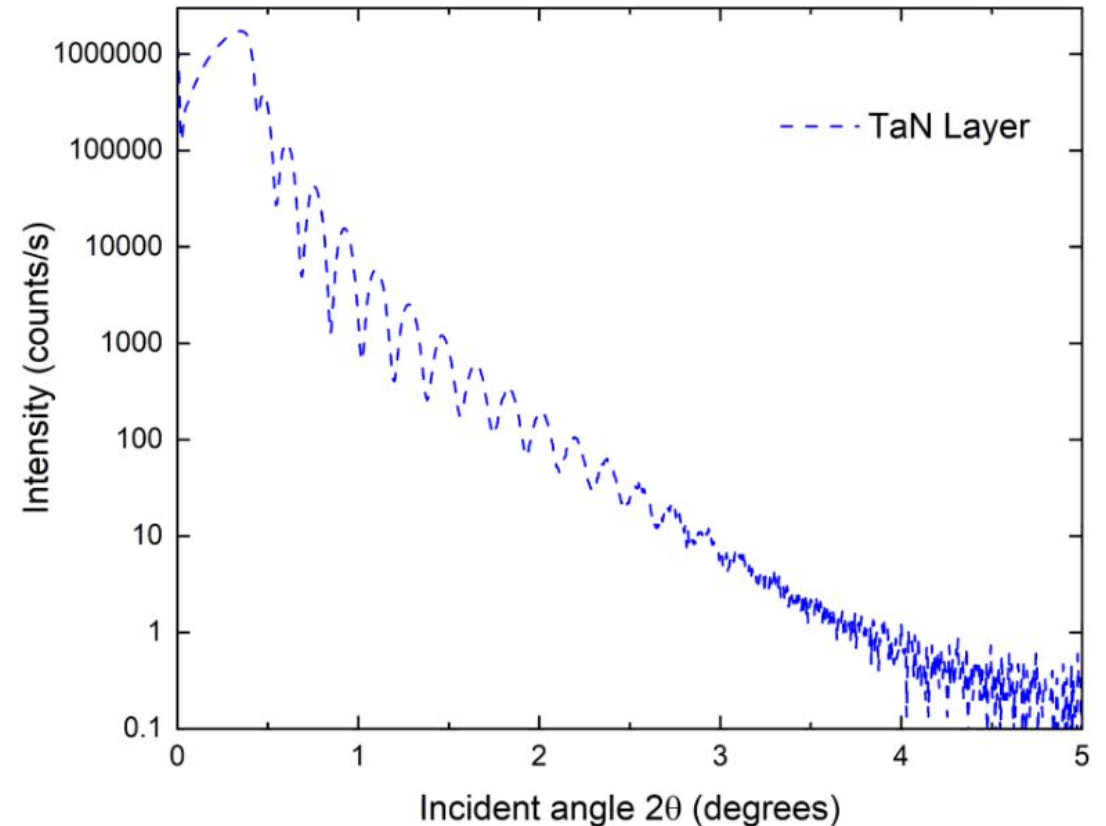

PANalytical Empyrean Powder Diffractometer (for XRR)

Malvern Panalytical, Empyrean, https://www.malvernpanalytical.com/empyrean
M. Yasaka, The Rigaku Journal, 26 (2), 1-9 (2010).
M. R. Sardela, Practical Materials Characterization (pp. 1-41), Media New York, 2014.

Methods pt. 2

Critical angle (deg)		Intensity (counts/s)	
0.415		873340.4	
Angle peak (deg)	Angle valley (deg)	Intensity (counts/s)	
	0.445		232286.1
0.475		396213.1	
	0.545		27097.6
0.605		121914.4	
	0.69		4966.5
0.755		42754.2	
	0.845		1290.5
0.925		15486.1	
	1.02		645.4
1.095		5863.1	
	1.2		404.6

Since the software did not have a layer for TaN, we had to create it from scratch, editing a layer and adding Tantalum and Nitrogen with the default settings for each of them.

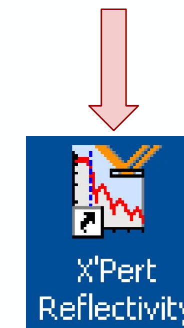

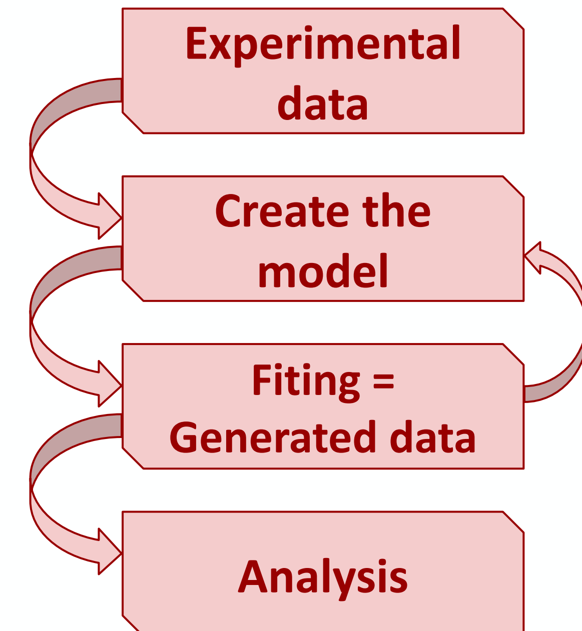

Malvern Panalytical, Empyrean, https://www.malvernpanalytical.com/empyrean
M. Yasaka, The Rigaku Journal, 26 (2), 1-9 (2010).
M. R. Sardela, Practical Materials Characterization (pp. 1-41), Media New York, 2014.

Methods pt. 3

	θ (deg)	q (nm^{-1})
Critical angle	0.415	32.900 ± 0.01
First peak	0.475	37.319 ± 0.01
Second peak	0.605	46.411 ± 0.01
Third peak	0.755	55.919 ± 0.01
Fourth peak	0.925	65.167 ± 0.01
Fifth peak	1.095	72.536 ± 0.01

$$q = q_z = \frac{4\pi}{\lambda} \sin\theta$$

reciprocal space coordinate

$$T = \frac{\lambda}{2 * \Delta\theta} = \frac{2\pi}{\Delta Q}$$

Oscillations	Δθ (deg)	ΔQ (nm^{-1})
1st-2nd peak	0.130	9.092 ± 0.014
2nd-3rd peak	0.150	9.508 ± 0.014
3rd-4th peak	0.170	9.248 ± 0.014
4th-5th peak	0.170	7.369 ± 0.014
Average spacing	0.155	8.804 ± 0.014

Malvern Panalytical, Empyrean, https://www.malvernpanalytical.com/empyrean
M. Yasaka, The Rigaku Journal, 26 (2), 1-9 (2010).
M. R. Sardela, Practical Materials Characterization (pp. 1-41), Media New York, 2014.

Results

$$\delta = \frac{r_e}{2\pi}\lambda^2\rho_e = \frac{N_A Z r_e \mu}{2\pi A}\lambda^2 \qquad \theta_{crit} \approx \sqrt{2\delta} \qquad T = \frac{\lambda}{2*\Delta\theta} = \frac{2\pi}{\Delta Q}$$

- Electron density was calculated as: 3.7919 $\pm$ 0.0029*10^{24} cm^{-3}, considering the value for delta as 2.621 $\pm$ 0.002*10^{-5}.
- The molar mass, A, of TaN is 194.955 $\pm$ 0.00022 g/mol.
- The sum of its atomic number is 80 (73 for Ta + 7 for N).
- The mass density of the TaN layer is 9.9643 $\pm$ 0.0076 g/cm^3.
- The average spacing between the first four oscillations was 0.155^o or 0.002705 radians.
- The thickness for the TaN layer was calculated to be 28.52 $\pm$ 0.02 nm.
- While roughness causes the decay of the XRR signal at higher angles, the exact rate of decay is dependent on a complex interplay of other factor apart from the slope, so it requires a specialized software for analysis.

Results pt. 2

	Density (g/cm^3)	Thickness (nm)	Roughness (nm)
ZincBlende, TaN	9.776 $\pm$ 0.005	23.478 $\pm$ 0.005	0.349 $\pm$ 0.005

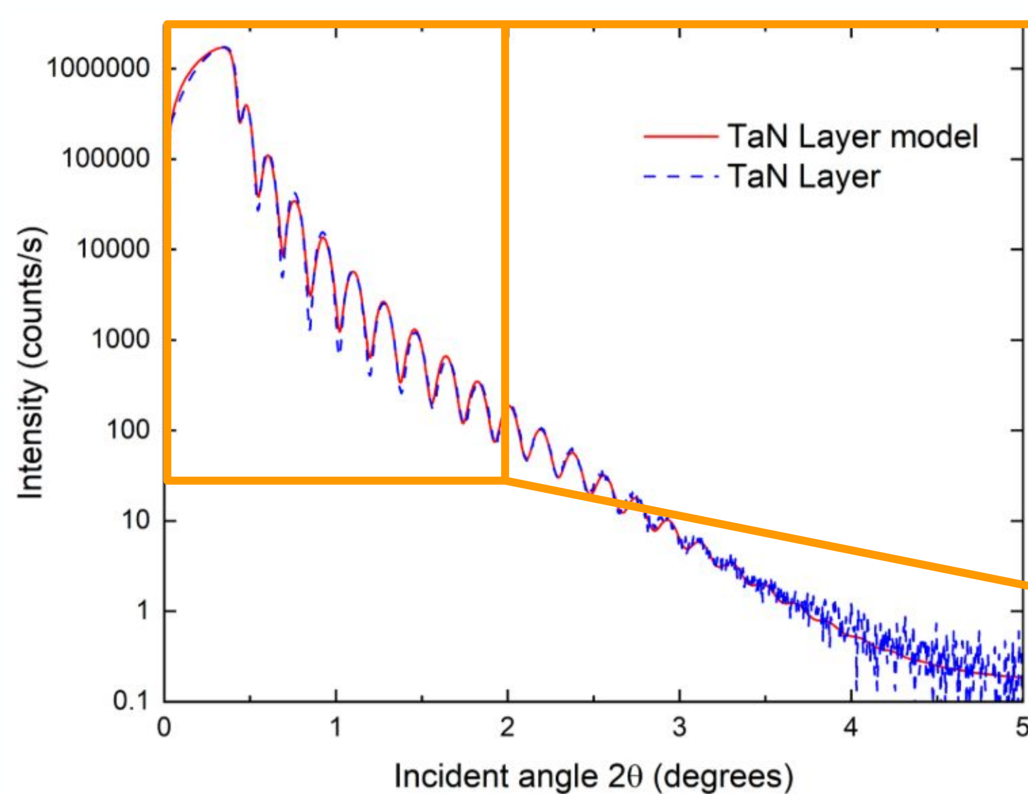

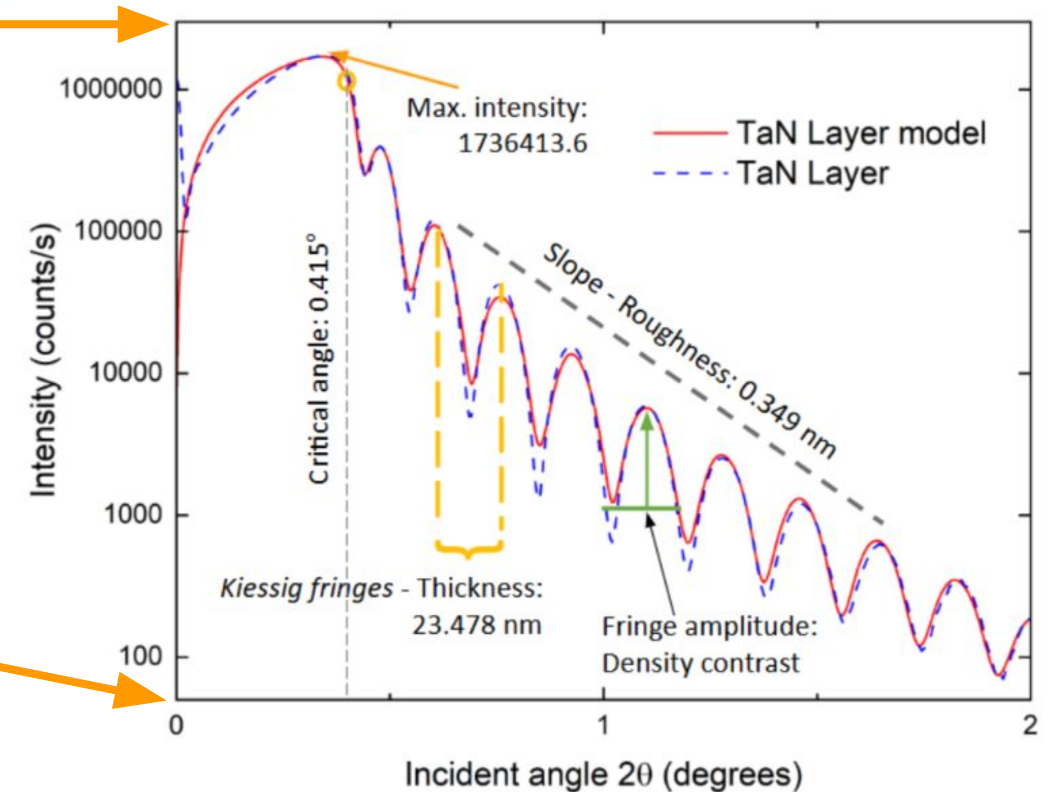

Conclusion

Note: Although this thesis includes this XRR chapter before the ellipsometric measurements, the work done with XRR was performed at the very end of the project.

	Density (g/cm^3)	Thickness (nm)	Roughness (nm)
TaN, experimental	9.9643 ± 0.0076	28.52 ± 0.02	-----
TaN, model	9.776 ± 0.005	23.478 ± 0.005	0.349 ± 0.005

For the density of the layer, there is a difference of 0.1883 ± 0.009 g/cm^3, which shows a good coherence of the model to describe the experimental data.
For the thickness of the layer there is a difference of 5.042 ± 0.021 nm, which represents a not too large but still noticeable variation in layer thickness that can be attributed to the limited use of fringes when manually calculating the average fringe spacing.

- Critical angle = 0.415^{o}

The angle range of 0.7^{o} to 1.7^{o} of the XRR pattern shows a slight difference in amplitude between the experimental data and the model, which can be attributed to the sample having more than one layer. This is something that can be worked on in a future experiment, trying to fit a model, and adding more layers for TaN.

Temperature-dependent dielectric function of tantalum nitride formed by atomic layer deposition for tunnel barriers in Josephson Junctions

Introduction

- Superconducting qubits, such as those based on Josephson junctions, rely heavily on the quality of their insulating tunnel barriers. Traditionally, these barriers are made using AlO_x, but that approach faces challenges — especially with uncontrolled oxidation, variability in stoichiometry, and limitations in scaling.
- Here's where **ALD TaN** comes in: This material offers atomic-level control during deposition, excellent uniformity across large wafers, and compatibility with CMOS fabrication — all crucial for scalable quantum devices.
- However, despite TaN's established use in microelectronics as a diffusion barrier, its **optical and dielectric properties at different temperatures** had not been fully characterized — and that's exactly what this research set out to explore.

BE BOLD. Shape the Future.®

Morten Kjaergaard et al., Annual Rev. of Cond. Mat. Phys., 11, 369–395 (2020).
W. D. Oliver, and P. B. Welander, MRS Bulletin 38, 816-825 (2013).
G.Wendin and V. S. Shumeiko, Low Temp. Phys., 33, 724–744 (2007).
J. M. Martinis et al., Physical Review Letters, 95, 210503 (2005).
A. P. M. Place et al., Nature Communications 12, 1779 (2021).

Psi and Delta of SiO_2

Ellipsometric angles Psi and Delta as a function of Photon Energy for the center, middle, and edge sections of the wafer at 300 K before ALD TaN.

The angle of incidence was limited to 70°

Layer thickness in all sections: 44 nm

Create a layer **model for the oxide** of the thin film to fix it when fitting the model for the TaN surface layer.

The model for the SiO_2/Si layer was made using 2 Gaussian oscillators around 0.05 and 0.12 eV.

The models for all 3 sections of the wafers are basically identical.

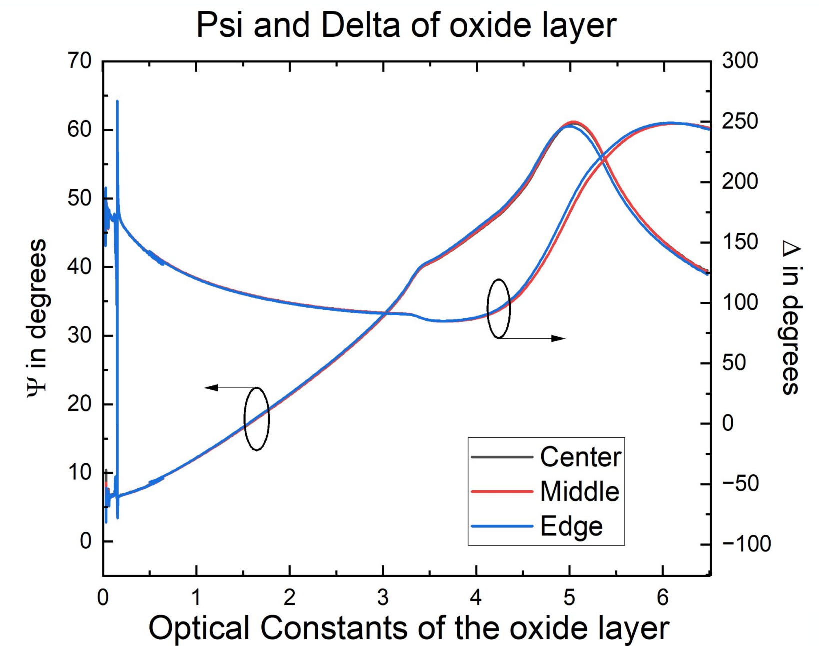

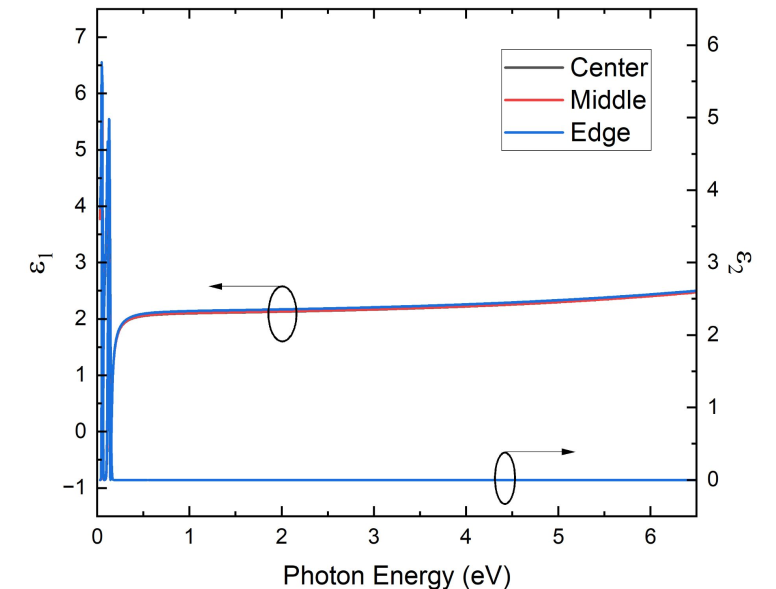

G. E. Jellison, Jr., and F. A. Modine, Appl. Phys. Lett. 69, 371 (1996); 69, 2137 (1996) (E).

Psi and Delta of TaN

Ellipsometric angles Psi and Delta as a function of Photon Energy for the 25 nm TaN center sample at room temperature (300 K)

Range of angles: 50° to 80°, step size: 5°

± polarizer angles

Brewster angles:

Si: 75° SiO_2: 55°

IR (0.03 to 0.7 eV):

Resolution: 8 cm^{-1}

UV (0.5 to 6.5 eV):

Energy step size: 0.02 eV

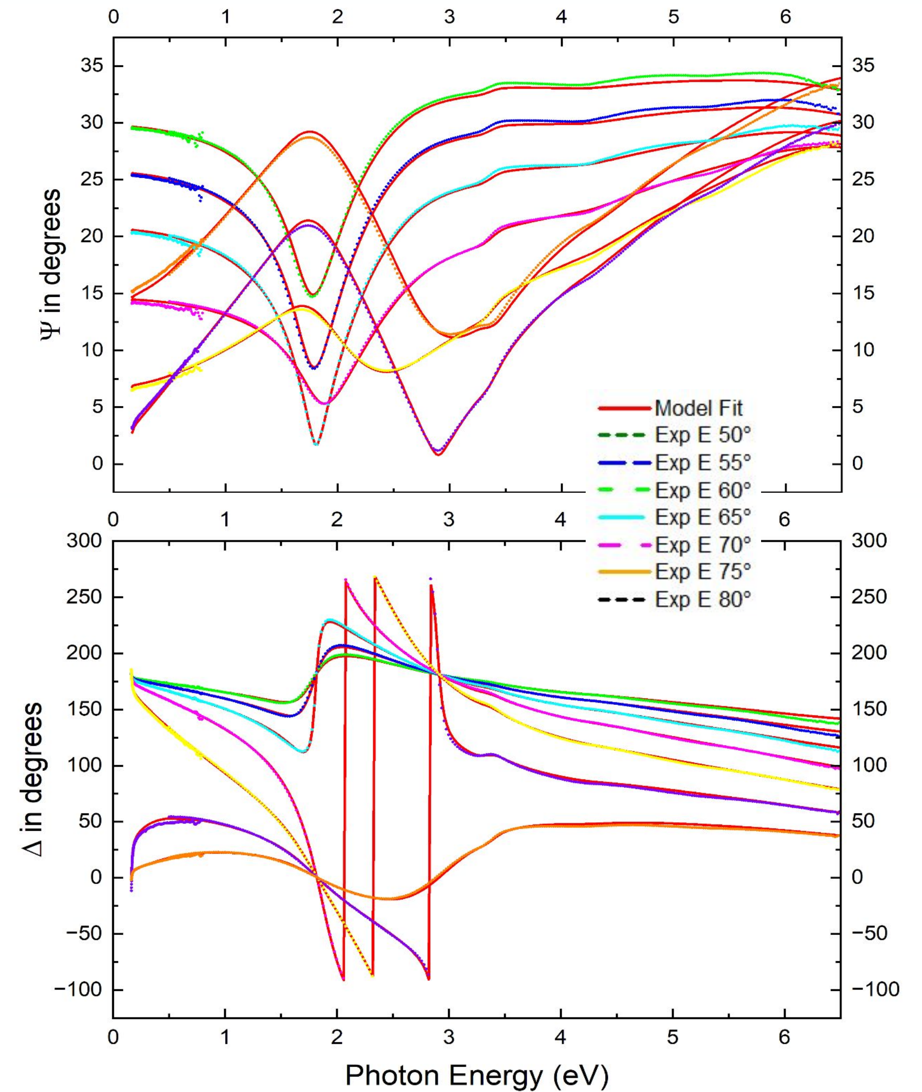

G. E. Jellison, Jr., and F. A. Modine, Appl. Phys. Lett. 69, 371 (1996); 69, 2137 (1996) (E).

Pseudo dielectric functions of TaN

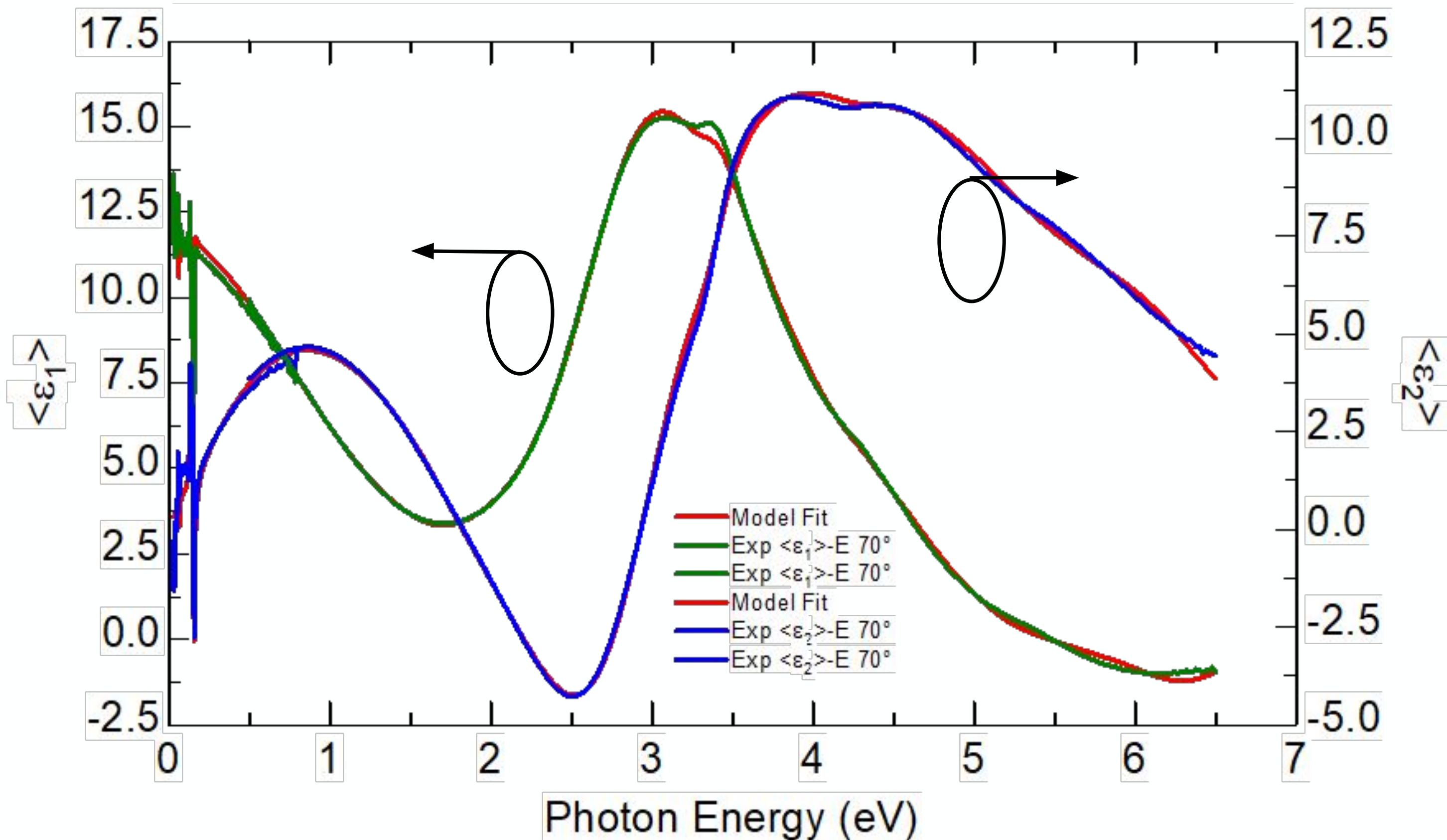

Angle of incidence fixed at 70°

IR:

Resolution: 8 cm^{-1}

UV:

Energy step size: 0.02 eV

TaN layer model:

-1 Tauc-Lorentz oscillator at 3.2 eV

-2 Gaussians at 0.44 and 4.8 eV

-Fixed thickness: 23 nm

Absorption peak: 2.5 - 6.5 eV

Interference fringe below 2.5 eV

-Half the size of absorption peak

G. E. Jellison, Jr., and F. A. Modine, Appl. Phys. Lett. 69, 371 (1996); 69, 2137 (1996) (E).

Diff. thicknesses assumed for SiO_2

- Broad range of SiO_2 thicknesses ranging from 35 to 52 nm.
- An SiO_2 thickness of 44 nm yields leads to a peak in the dielectric function of TaN near 1.2 eV.
- The magnitude of this peak increases if we assume an SiO_2 thickness of 52 nm.
- It nearly disappears for a SiO_2 thickness of 35 nm.

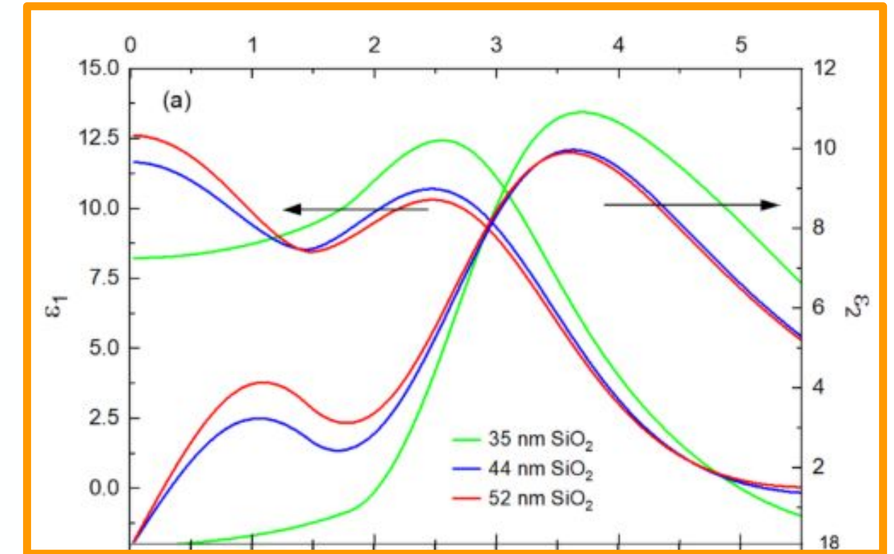

- The strong dependence of the peak at 1.2 eV on the SiO_2 thickness in our fit is suspicious. Most likely, this peak is an artifact that stems from an incomplete removal of interference effects.
- Since this peak disappears if we assume an SiO_2 thickness of 35 nm, this is the most likely scenario and we fix it in our subsequent analysis work.

G. E. Jellison, Jr., and F. A. Modine, Appl. Phys. Lett. 69, 371 (1996); 69, 2137 (1996) (E).

Temperature dependence of TaN

The temperature dependence of the dielectric function of TaN is small. The band gap of TaN (more precisely, the Tauc gap extracted from our Tauc-Lorentz oscillator model) decreases from 1.8 eV at 80 K to 1.5 eV at 600 K.

Furthermore, as expected, the broadening of the main peak around 3.5 eV increases with increasing temperature.

The imaginary part of ε remains small at all temperatures, indicative of the insulating properties of the TaN layer.

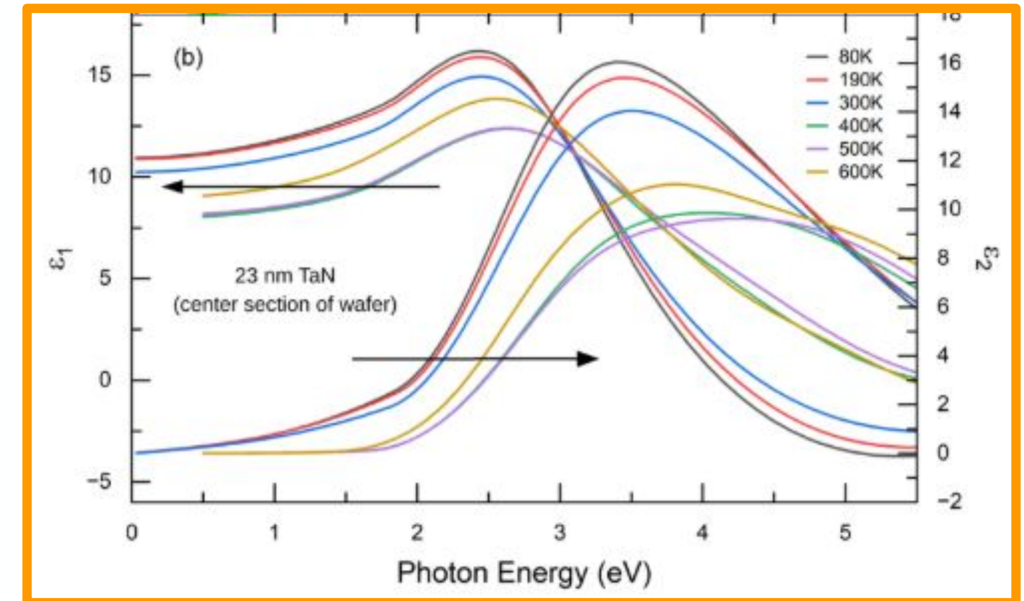

S. Zollner et al., Advanced Optical Technologies 11, 117-135 (2022).
D. Franta et al., Appl. Surf. Sci. B 421, 405 (2017).
D. Franta, P. Franta, J. Vohánka, M. Čermák, and I. Ohlídal, J. App. Phys. 123, 185707 (2018).

NM STATE BE BOLD. Shape the Future.®

Dielectric functions of TaN in diff. thicknesses

$$A = \ln\left(\frac{I_o}{I}\right) = \alpha d$$

Beer-Lambert law: the decrease in the intensity of light as it passes through a medium is an exponential function of the distance it travels.

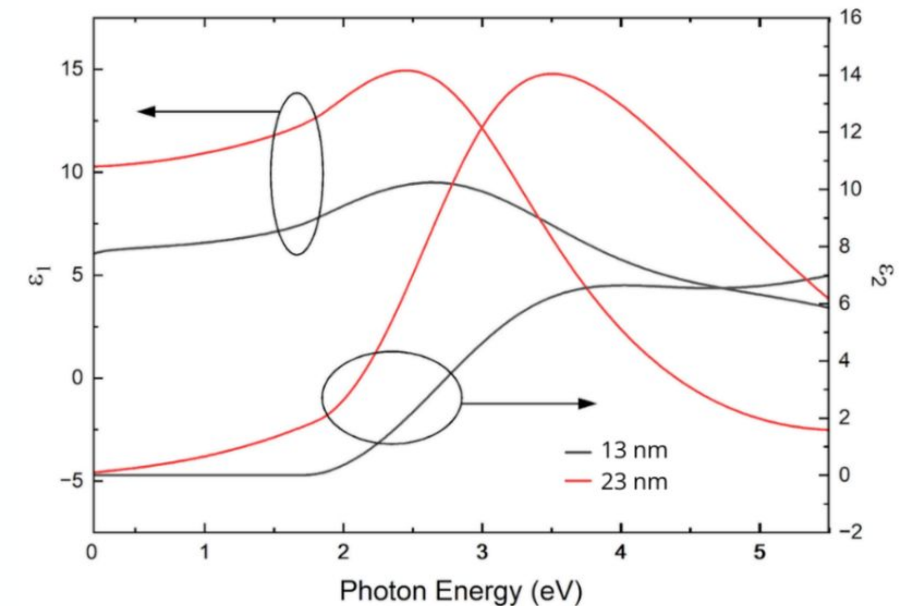

- Because the thinner sample's film thickness is approximately half of the thicker sample, the absorbance was also halved while the absorption coefficient remained the same.
- The 13 nm sample could be almost completely oxidized forming some type of TaxOx which made its absorption coefficient different, therefore, changing its dielectric functions.
- Excitonic enhancement, which is where excitons, bound states of electrons and holes, significantly modify a material's optical properties, like the absorption coefficient, due to the attractive Coulomb interaction between the electron and hole.

Comparison of diff. sections of TaN wafers

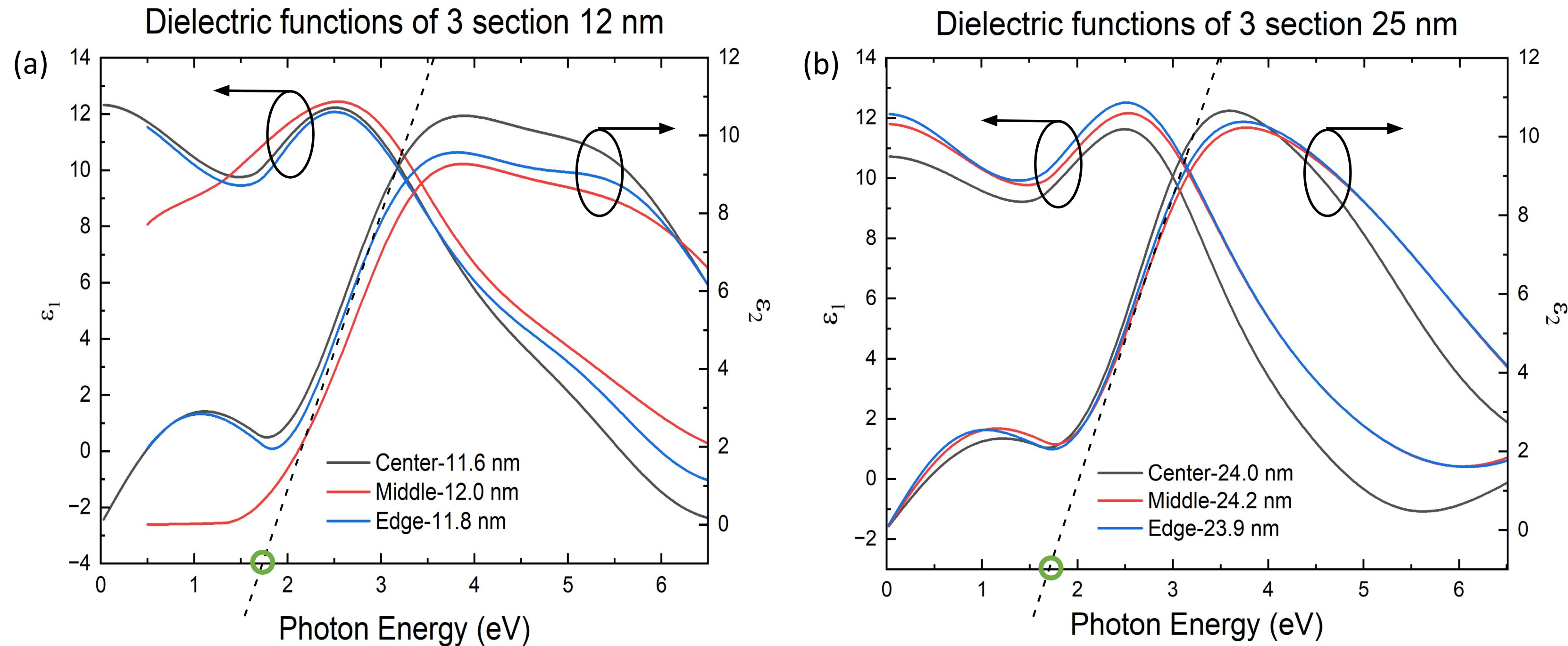

Band gap of TaN: ∼1.7 eV

The imaginary part of the dielectric function of the three sections in both graphs shows a band gap near 1.7 eV at room temperature, which confirms the desired objective of maintaining uniform optical constants throughout the wafer.

Since these two graphs were made using a TaN model on top of an SiO_2 model that considered a thickness of 40 nm instead of 35 nm, it is possible these peaks are due to an artifact caused by an incomplete removal of the interference fringe.

Conclusion

We explored the application of ALD TaN films for tunnel barriers in Josephson junctions for superconducting quantum circuits.

- The ALD TaN band gap was determined to be 1.5-1.8 eV varying with temperature. This showed:
  - No evidence for free-carrier absorption in the infrared region (consistent with the insulating nature of the ALD TaN film)
  - Its advantages over traditional aluminum oxide barriers of higher band gap used in tunnel barriers
  - That the smaller barrier height allows for thicker films to be utilized for the same magnitude of Josephson tunneling current, improving process control margin.
  - The excellent surface roughness and band gap uniformity across the 300 mm wafer that illustrates ALD TaN as a potential material for Josephson junctions to achieve thermally stable, reliable, and repeatable superconducting qubit devices.

Future work will focus on the determination of dielectric loss in ALD TaN and its integration as tunnel barriers into Josephson junctions and the determination of coherence times of superconducting qubit devices made from these Josephson junctions.

Outlook and Summary

C25
C12
Wafer ID: 46KAV139SJC6 (Si/SiO₂(post Ar-sp)/ALD TaN(25nm))
JC6-C25 JC6-M25 JC6-E25
JF7-C12 JF7-M12 JF7-E12
Wafer ID: 46KAV138SJF7 (Si/SiO₂(post Ar-sp)/ALD TaN(12nm))
Wafer ID: 46KAS017SJH1 (Si/SiO₂(post Ar-sputter))
JH1-Cox JH1-Mox JH1-Eox
JE4-C50 JB3-Csi
Wafer ID: 46KAV127SJE4 (Si/SiO₂(as grown))
Wafer ID: 46KAV130SJB3 (Si substrate)

BRANSON
Ultrasonic cleaner

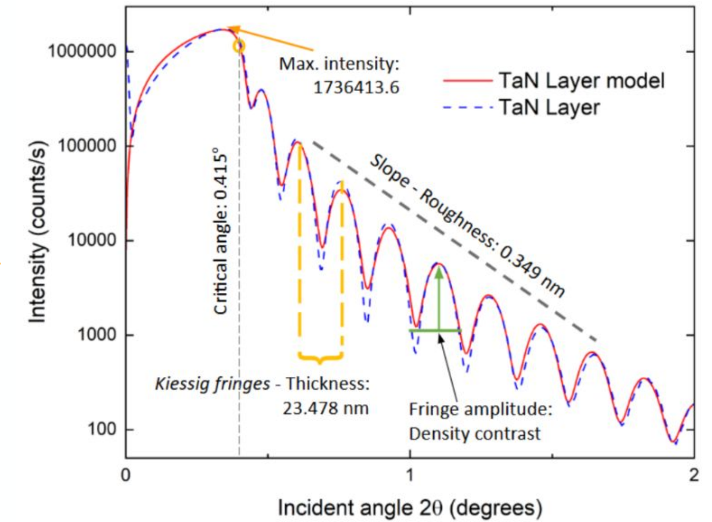
Max. intensity: 1736413.6
TaN Layer model
TaN Layer
Critical angle: 0.415°
Slope - Roughness: 0.349 nm
Kiessig fringes - Thickness: 23.478 nm
Fringe amplitude: Density contrast
Intensity (counts/s)
Incident angle 2θ (degrees)

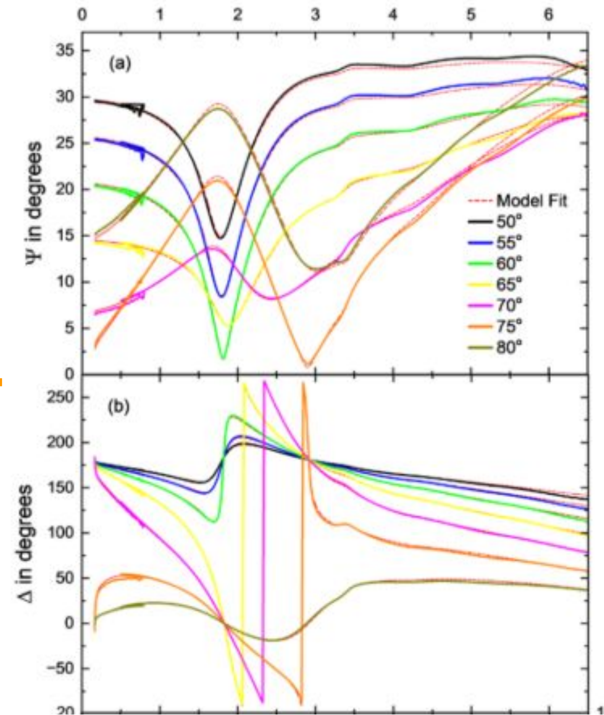
(a)
Ψ in degrees
Model Fit
50°
55°
60°
65°
70°
75°
80°
(b)
Δ in degrees

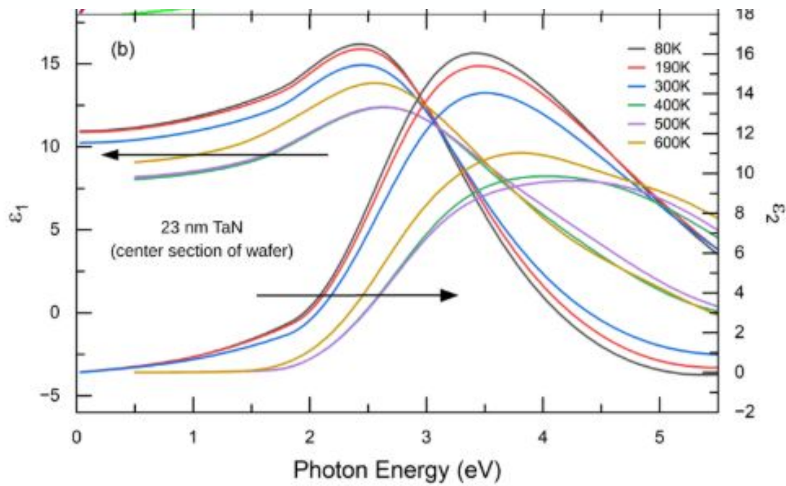
(b)
80K
190K
300K
400K
500K
600K
23 nm TaN
(center section of wafer)
Photon Energy (eV)

Outlook and Summary

- XRR on ALD TaN showed a critical angle of 0.415^{o}, a layer thickness of 23.478 nm, a surface roughness of 0.349 nm, and a layer density of 9.776 g/cm^3.
- The band gap for the ALD TaN thin film was found from 1.8 eV to 1.5 eV varying with temperature from 80 K to 600 K.
- ALD TaN has some variation in its optical constants due to temperature, especially around the energies corresponding to the absorption peaks (3.5 and 5 eV).
- Leveling the parallel abrupt interfaces with well known thicknesses will improve the measured SE data.

Thank you!

BE BOLD. Shape the Future.®

Questions?

BE BOLD. Shape the Future.®